

SIT004-01

会場:105

時間:5月25日 10:45-11:15

A discussion on the cause of high electrical conductivity in the oceanic upper mantle A discussion on the cause of high electrical conductivity in the oceanic upper mantle

歌田 久司^{1*}, 馬場 聖至¹
Hisashi Utada^{1*}, Kiyoshi Baba¹

¹ 東京大学地震研究所

¹ERI, University of Tokyo

Distribution of electrical conductivity in the oceanic upper mantle is estimated by inverting electromagnetic data obtained regionally by an array of electric and magnetic field measurements in the ocean basin. Then physical interpretation is made, sometimes jointly with seismological parameters, by referring to results of mineral physics. There are a number of possible ways to invert regional electromagnetic data in the form of one-dimensional (1-D), 2-D and 3-D models. Among them, the regionally averaged 1-D profile provides a mean feature of the study region and is considered as conservative but robust estimate that can be extracted from a regional observation. Here we show most recent result of seafloor EM study carried out in the Philippine Sea and western Pacific regions, installing total of 39 sites for 3 years (2006-2008) in the Stagnant Slab Project (Baba et al., 2010). Both profiles show high conductivity of about 0.3-0.5 S/m in the upper mantle under a low conductivity layer. The Philippine Sea profile reaches this value at the depth of 60-70 km, while it is about 200 km depth for the western Pacific profile. These two profiles are almost identical at depths greater than 200 km and down to the top of the transition zone. Baba et al. (2010) discussed the differences in these two conductivity profiles by considering the seafloor age (geothermal), the degree of (silicate) partial melt, and the water content. In this paper we make further discussion on the cause of the high conductivity in the upper mantle in terms of effects of silicate and carbonatite partial melts with reference to recent experimental results (Gaillard et al., 2008; Yoshino et al., 2010). We also refer to the calculation of the stability of partial melts by Hirschmann (2010), and examine whether observed profiles can be explained by the effect of partial melts and by existing knowledge. The two experimental results are not completely consistent with each other, and therefore lead us to different conclusions as follows:

(a) Yoshino et al. (2010) presented a diagram showing the melt fraction dependence of electrical conductivity of partially molten mantle both for silicate and carbonatite melts. We directly compared it to our observation and found that the high conductivity at 60-70 km depth of Philippine Sea result can be explained by 0.5 % partial silicate melt. However, if we take the melt fraction of 0.024 % at the boundary between stability regions of silicate and carbonatite melts (Hirschmann, 2010), conductivity values are expected to be as low as that of dry olivine, and therefore inconsistent to the observed profile.

(b) We calculated the melt fraction dependence of the partially molten mantle conductivity based on Gaillard et al. (2008), by assuming the Hashin-Strickman upper bound model. From this diagram, the high conductivity values both at 60-70 km and at 200 km can be explained by partially molten mantle either with 2-3 % silicate melt or with 0.02-0.04 % carbonatite melt. Explaining the observed profiles by the effect of partial silicate melt requires too high melt fraction and therefore seems difficult. On the other hand, observed profiles may be explained by the effect of partial carbonatite melt with melt fraction that could be stable at respective depths. However in this case, the consistency with seismological evidence (e.g. Kawakatsu et al., 2009) may still remain a problem.

Such a comparison as shown above does not give us a solid conclusion because of still insufficient knowledge. However, it is possible for us in principle to constrain a product of the melt fraction and the melt conductivity from electrical conductivity profiles. Furthermore if the melt fraction is constrained somehow by seismological observations, for example, electrical conductivity profiles will consistently constrain the melt conductivity, from which the volatile content in the melt that is responsible for the high conductivity can be inferred.

Keywords: oceanic upper mantle, electrical conductivity, ocean bottom observation, partial melt

SIT004-02

会場:105

時間:5月25日 11:15-11:45

H₂O storage capacity of the upper mantle and melting atop the 410 km discontinuity H₂O storage capacity of the upper mantle and melting atop the 410 km discontinuity

Marc Hirschmann^{1*}

Marc Hirschmann^{1*}

¹University of Minnesota

¹University of Minnesota

There is considerable evidence that partial melts are stable in regions of the upper mantle that are deeper than the plausible locus of dry melting of peridotite, and this is widely recognized to mean that volatile-enhanced melting is a common phenomenon in the convecting upper mantle. Among the most enigmatic of these regions are low shear-wave velocity regions atop the 410 km discontinuity, which are widespread regional features. Numerous seismic studies, principally using receiver functions and ScS reverberations, have detected anomalously slow regions in the 20-80 km thick interval above the 410 km discontinuity. Because these regions are commonly 3-8% slow relative to reference models, it is difficult to explain them without the presence of interstitial melt. Alternative explanations, such as enhanced hydration of nominally anhydrous minerals, do not seem to be able to account for the magnitude of the observed anomalies. Many, though not all, of the low velocity zones are associated with regions of present or recent subduction, suggesting that they mark regions of partial melt incited by advection of recycled volatiles into the upper mantle. H₂O and CO₂, alone or in combination, may be capable of inciting partial melting at these depths. Because the convecting mantle is reduced at these depths, and because CO₂ solubility in melts under reducing conditions is very small, CO₂ contributes negligibly to melt stabilization unless the low velocity regions are anomalously oxidized. Thus, hydrous melting is the most likely explanation for the observations.

Hydrous melting atop the 410 km discontinuity can occur if the local concentration of H₂O exceeds the storage capacity of peridotite. The storage capacity is the maximum concentration of H₂O that can be held in the nominally anhydrous minerals at a given temperature and pressure for the chemical system of interest. A critical point, therefore, is that the storage capacity will depend on the diversity and compositions of phases present. The concentrations of H₂O that can be stored in olivine at 12-14 GPa along the mantle adiabat approach 0.5 wt.%, but the presence of the full peridotite mineral assemblage stabilizes partial melt at diminished H₂O activity and severely reduces the H₂O storage capacity. New experiments conducted at 10-13 GPa indicate that olivine saturated with peridotite and with hydrous partial melt has 500-1800 ppm H₂O. These concentrations are similar to those that might be expected in recycled oceanic lithosphere at TZ depths or in plumes and are consistent with the hydrous melting hypothesis to explain regional observations of LVZ at 410 km. However, they are considerably greater than concentrations in typical convecting mantle sampled at ridges, and are therefore inconsistent with a global layer of melt at 410 km. Remaining challenges include accounting for the unexpectedly great thickness of observed layers, and constructing a petrologically and dynamically consistent explanation for the magnitude of shear wave anomalies, which are not easily reconciled with the fractions of melt that are petrologically likely or dynamically stable.

キーワード: Transition Zone, 410 km discontinuity, hydrous melting

Keywords: Transition Zone, 410 km discontinuity, hydrous melting

SIT004-03

会場:105

時間:5月25日 11:45-12:00

Laboratory-based electrical conductivity profile of the mantle transition zone Laboratory-based electrical conductivity profile of the mantle transition zone

芳野 極^{1*}, 桂 智男², 下宿 彰¹

Takashi Yoshino^{1*}, Tomoo Katsura², Akira Shimojuku¹

¹ 岡山大学地球物質科学研究センター, ²BGI, Univ. Bayreuth

¹ISEI, Okayama Univ., ²BGI, Univ. Bayreuth

Recent laboratory electrical conductivity measurements of the main mantle constituent minerals have refined our understanding of the effect of water and iron content on electrical conductivity. However, there have remained inconsistency of conductivity data between different laboratories, especially effect of water on the conductivity (proton conduction). Karato and Dai (2009) claimed that our group's data, mostly based on low frequency measurements, used incorrect sample conductivity values, because their impedance spectroscopy for wet wadsleyite measured at high temperatures showed an additional tail at low frequencies. To clarify a cause of this discrepancy, we performed the impedance spectroscopic measurements for wadsleyite in a wide frequency range at low temperatures (< 1000 K) to minimize dehydration of samples. The results are quite consistent with ours measured at low frequencies, and did not show a large contribution of small amount of water to the conductivity and an additional tail at low frequencies due to the electrode reaction. It is concluded that the conductivity measurement at high temperatures (> 1000 K) leads to higher conductivity due to the grain boundary water generated by dehydration of sample.

Next we consider the electrical conductivity structure of the mantle transition zone based on our results. The electrical conductivity of the Earth's mantle is controlled by the coexistence of multiple mineral phases. Using these conductivity data of mantle minerals and geotherm models, the laboratory-based conductivity-depth profiles have been constructed of a 200 to 800 km depth range across the mantle transition zone. These profiles are based on mixing models of composite materials, which assume a pyrolytic composition, and they are a function of water content in main constituent minerals. The calculated conductivity values increase from 10-2 S/m at 200 km depth to 100 S/m at 800 km depth. Considering the conductivity change due to the phase change only, our model predicts similar values between olivine and wadsleyite, but they differ up to nearly one order of magnitude between wadsleyite and ringwoodite. In other words, if a conductivity jump accompanies the 410 km seismic discontinuity, it will not be due to the phase change but to a secondary effect, such as difference in water content. Instead, a notable conductivity jump appears at a depth of 520 km in the wadsleyite-ringwoodite transition with or without water. The present conductivity-depth profile in the transition zone agrees with that obtained from the geophysical observations beneath the Pacific Ocean in the case of the dry mantle transition zone. The absolute conductivity values obtained from the conductivity profiles beneath the Philippine Sea, where stagnant slab exists, are too high to be explained by the dry pyrolytic model, especially in the stability field of wadsleyite. Presence of water in the transition zone minerals is required to explain such high conductivity.

Keywords: electrical conductivity, mantle transition zone, water, olivine, wadsleyite, ringwoodite

SIT004-04

会場:105

時間:5月25日 12:00-12:15

マントルの不均質構造と異方性のイメージング Mapping seismic heterogeneity and anisotropy in the mantle

趙 大鵬^{1*}

Dapeng Zhao^{1*}

¹ 東北大学・理

¹Tohoku University

Recently we have made new advances in tomographic imaging of the mantle heterogeneity and anisotropy, which shed new light on the mantle dynamics. We improved our global tomography model by adopting a flexible-grid parameterization to express the 3-D Earth structure (Zhao, 2009). Compared with the previous tomographic model (e.g., Zhao, 2004), the new model has a better resolution for the polar regions, which enables us to examine the mantle structure and dynamics in Arctic and Antarctica. The intraplate volcanoes in NE Asia (e.g., Changbai and Wudalianchi) are caused by the hot and wet upwellings in the big mantle wedge (BMW) above the stagnant slab in the mantle transition zone (Zhao, 2004; Zhao et al., 2009). Our new tomography model shows that the subducting Pacific slab becomes stagnant in the mantle transition zone under Western Alaska, Bering Sea, Sea of Okhotsk, Japan Sea, and Northeast Asia. Many intraplate volcanoes exist in these areas, which are located above the low-velocity zones in the upper mantle above the stagnant slab, suggesting that BMW exists in not only NE Asia but also in broad regions under the northern and western Pacific, and those intraplate volcanoes are related to the dynamic processes in the BMW above the stagnant slab. The Tengchong volcano in SW China is caused by a similar process in BMW above the subducting Burma microplate (or Indian plate). In contrast, the Hainan volcano in southernmost China is a hotspot fed by a lower-mantle plume associated with the Pacific and Philippine Sea slabs' deep subduction in the east and the Indian slab's deep subduction in the west down to the lower mantle (Zhao et al., 2011). We have also used P-wave anisotropy tomography and shear-wave splitting to map seismic anisotropy in the mantle under East Asia. The results show that the fast velocity direction in the upper mantle under East Asia is generally oriented in the NW-SE or E-W directions, suggesting the existence of mantle flow in the BMW, in consistent with the tomographic images and stress regime in the subducting slab as estimated from the focal mechanism solutions of deep earthquakes under the Japan Sea and East-Asia margin (Zhao et al., 2009, 2011).

References

- Zhao, D. (2009) Multiscale seismic tomography and mantle dynamics. *Gondwana Res.* 15, 297-323.
Zhao, D., Y. Tian, J. Lei, L. Liu (2009) Seismic image and origin of the Changbai intraplate volcano in East Asia: Role of big mantle wedge above the stagnant Pacific slab. *Phys. Earth Planet. Inter.* 173, 197-206.
Zhao, D., F. Pirajno, N. Dobretsov, L. Liu (2010) Mantle structure and dynamics under East Russia and adjacent regions. *Russ. Geol. Geophys.* 51, 925-938.
Zhao, D., S. Yu, E. Ohtani (2011) East Asia: Seismotectonics, magmatism and mantle dynamics. *J. Asian Earth Sci.*, 40, 689-709.

キーワード: マントル, 不均質, 異方性, スラブ, 深発地震

Keywords: mantle, heterogeneity, anisotropy, slab, deep earthquakes

SIT004-05

会場:105

時間:5月25日 12:15-12:30

Elastic wave velocities of stishovite at high pressures Elastic wave velocities of stishovite at high pressures

根岸 嶺^{1*}, 河野 義生¹, 肥後 祐司², 西山 宣正¹, 入舩 徹男¹
Ryo Negishi^{1*}, Yoshio Kono¹, Yuji Higo², Norimasa Nishiyama¹, Tetsuo Irifune¹

¹ 愛媛大学地球深部ダイナミクス研究センター, ²(財) 高輝度光科学研究センター

¹Geodynamics Research Center, Ehime Univ., ²Japan Synchrotron Radiation Research Ins

Stishovite is an important constituent of the Earth's mantle transition region, and therefore elastic wave velocity of stishovite, in conjunction with seismological observations, should give constraints on the mineralogy of the mantle transition region. Previous studies have measured elastic wave velocities of stishovite at high pressures to 3 GPa by ultrasonic technique (Li et al., 1996) and to 12 GPa by Brillouin scattering measurement (Jiang et al., 2009). However, the results are inconsistent each other. In addition, these studies were carried out at pressures lower than that of mantle transition region. We therefore need further elastic wave velocity measurement of stishovite at the pressure and temperature conditions of the mantle region.

Here we carried out elastic wave velocity measurement on sintered polycrystalline stishovite from 10.3 GPa to 17.5 GPa at room temperature by using ultrasonic technique in conjunction with synchrotron X-ray measurement. The polycrystalline stishovite sample was hot pressed at ~16 GPa and ~1470 K in a 3000-ton Kawai-type apparatus using SiO₂ glass rod as starting material. The bulk density measured by Archimedes method before high pressure experiment was 4.29(2) g/cm³, which was same density as that determined by X-ray diffraction measurement (4.280 g/cm³).

Simultaneous ultrasonic and in situ X-ray measurements were carried out at BL0401 beamline in SPring-8. Ultrasonic elastic wave velocity measurements were conducted using the pulse reflection method. Sample lengths at high pressures were directly determined from the X-ray radiography image. Pressure was determined by self-consistent manner using obtained elastic wave velocity and density of stishovite.

Pressure-volume relation of stishovite measured in this study is consistent with these of previous studies (e.g. Lakshtanov et al., 2005; Nishihara et al., 2005). Our obtained elastic wave velocities of stishovite are higher than that of low pressure ultrasonic measurement to 3 GPa (Li et al., 1996). For instance, P wave velocity (VP) at 3 GPa estimated from our high pressure data is 12.02 km/s, but that of Li et al. (1996) less than 11.8 km/s. In contrast, our results are almost consistent with previous Brillouin scattering measurement on single-crystal stishovite up to 12 GPa (Jiang et al., 2009).

Keywords: stishovite, elastic wave velocity measurement

SIT004-06

会場:105

時間:5月25日 12:30-12:45

Diffusion of silicates in alkali carbonate melt and water fluid, experimental study at 17-24 GPa and 1400-1750°C

Diffusion of silicates in alkali carbonate melt and water fluid, experimental study at 17-24 GPa and 1400-1750°C

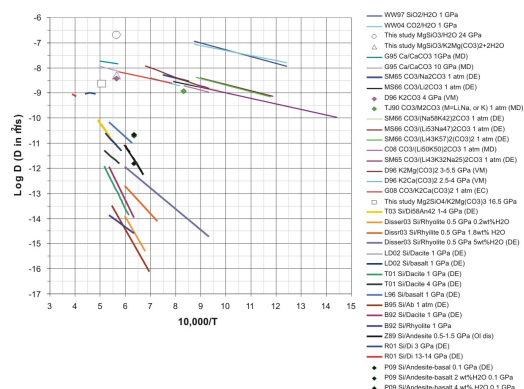
Anton Shatskiy^{1*}, Konstantin Litasov¹, Tomoo Katsura², Daisuke Yamazaki³, Eiji Ohtani¹
Anton Shatskiy^{1*}, Konstantin Litasov¹, Tomoo Katsura², Daisuke Yamazaki³, Eiji Ohtani¹

¹Tohoku University, ²Bayreuth Geoinstitut, Bayeruth, Germany, ³Okayama University

¹Tohoku University, ²Bayreuth Geoinstitut, Bayeruth, Germany, ³Okayama University

There are much direct and indirect evidences of carbonatitic and hydrous melt/fluid segregation in the deep mantle in the past Earth's history. One particular example is the source regions of carbonatites, kimberlites, and lamproites some of which originate from more than 250 km depth. Another example is the natural diamond forming medium which most probably was extremely enriched in water, carbonates, and alkalis. Despite of that, the average mantle concentrations of carbon and hydrogen do not exceed 100 and 120 wt ppm respectively, the volatile segregation in a broad mantle region should be involved to explain the local abundance of CO₂ and/or H₂O. Enrichment of these fluids in incompatible trace elements (specifically, K, Rb, Sr, Ba, light REE, Ti, Nb, Zr, P, U, and Th) also implies their long infiltration history through the large volumes of mantle rocks.

The probable mechanism of the fluid segregation in the deep mantle is the dissolution-precipitation mechanism. The rate of fluid segregation by this mechanism is proportional to the diffusion coefficient of silicate components in the fluid. Here we would like to present our current results on study of silicate diffusion in the K₂Mg(CO₃)₂, K₂Mg(CO₃)₂·2H₂O, and H₂O. The summary of obtained data is shown in the figure below along with available literature data on diffusion in the silicate and carbonate melts and water fluid.



キーワード: mantle, diffusion, carbonate, water fluid

Keywords: mantle, diffusion, carbonate, water fluid

SIT004-07

会場:105

時間:5月25日 14:15-14:30

P-V-T equation of state of the calcium aluminosilicate CAS phase, up to 24 GPa and 2100 K

P-V-T equation of state of the calcium aluminosilicate CAS phase, up to 24 GPa and 2100 K

Steeve Greaux^{1*}, Yoshio Kono¹, Norimasa Nishiyama¹, Tetsuo Irifune¹
Steeve Greaux^{1*}, Yoshio Kono¹, Norimasa Nishiyama¹, Tetsuo Irifune¹

¹Ehime University

¹Ehime University

The CAS phase is a Ca-rich aluminosilicate that has been first observed with the composition of $\text{Ca}_{0.8}\text{Al}_{3.6}\text{Si}_{2.4}\text{O}_{11}$ (with small amount of Na_2O and K_2O) in the decomposition product of sediments and continental crust composition at P,T conditions of mantle transition zone [1]. Later experiments also found the CAS phase as a liquidus phase in melting experiments on Mid-Ocean Ridge Basalts (MORB) compositions at 26-27 GPa and ~2500 K [2, 3]. According to those former studies, the CAS phase could represent up to 10 vol% of the subducted continental crust or 30 vol% of the solid fraction of partially molten MORBs in the deep mantle. Also, naturally occurring CAS phase has also been discovered in shocked martian meteorites [4]. Thus, the CAS phase might be an important constituent mineral of sediments and basalts subducted in the deep mantle.

The pressure-volume-temperature relations of the CAS phase with the composition of $\text{CaAl}_4\text{Si}_2\text{O}_{11}$ was examined in situ up to 24 GPa and 2100 K by energy dispersive X-ray diffraction, using a Kawai-type multi-anvil press apparatus coupled with synchrotron radiation in SPring-8 (Japan). At 300 K, we found that the CAS phase would be ~25% more compressible than Ono et al. [5]. From our high-temperature data we report for the first time the thermoelastic parameters of the CAS phase and discuss its compressibility and thermal expansivity relative to the lattice parameters variation at high-P,T.

These new data enables the accurate estimate of density of the CAS phase in the deep mantle for various temperature profiles (i.e. adiabatic mantle or cold slab geotherms). Our results suggest that with increasing the mineral proportion of the CAS phase, the density of slabs would increase when subducted in the mantle transition zone. On the other hand, because of lesser densities compared to lower mantle minerals, the CAS phase is expected to remain buoyant in the lowermost part of the transition zone.

References

- [1] Irifune et al., *Earth Planet. Sci. Lett.* 126(1994) 351-368.
- [2] Hirose and Fei, *Geochim. Cosmochim. Acta* 66(2002) 2099-2108.
- [3] Wang and Takahashi, *Am. Miner.* 84(1999) 357-361.
- [4] Beck et al., *Earth Planet. Sci. Lett.* 219(2004) 1-12.
- [5] Ono et al., *Phys. Earth Planet. Inter.* 150(2005) 331-338.

キーワード: CAS phase, $\text{CaAl}_4\text{Si}_2\text{O}_{11}$, Thermal expansion, high-pressure, in situ X-ray diffraction

Keywords: CAS phase, $\text{CaAl}_4\text{Si}_2\text{O}_{11}$, Thermal expansion, high-pressure, in situ X-ray diffraction

SIT004-08

会場:105

時間:5月25日 14:30-14:45

X線その場観察実験による Mg_2SiO_4 と $(\text{Mg}_{0.9}\text{Fe}_{0.1})_2\text{SiO}_4$ におけるポストスピネル相境界の決定

Determination of postspinel phase boundaries in Mg_2SiO_4 and $(\text{Mg}_{0.9}\text{Fe}_{0.1})_2\text{SiO}_4$ by in situ X-ray diffraction experiments

木下 夢^{1*}, 西山 宣正¹, 入船 徹男¹, 肥後 祐司², 舟越 賢一²

Yume Kinoshita^{1*}, Norimasa Nishiyama¹, Tetsuo Irifune¹, Yuji Higo², Ken-ichi Funakoshi²

¹ 愛媛大学 地球深部研, ² 高輝度光科学研究センター

¹Geodynamics Research Center, Ehime Univ, ²Japan Synchrotron Radiation Research Ins

We investigated postspinel phase boundaries in Mg_2SiO_4 and $(\text{Mg}_{0.9}\text{Fe}_{0.1})_2\text{SiO}_4$ between temperatures of 1673 and 2173 K by in-situ X-ray diffraction measurements at SPring-8. We did not observe effect of ferrous iron to the postspinel phase boundary, and they are expressed as $P \text{ (GPa)} = 26.42 - 0.0022 T \text{ (K)}$. The determined Clapeyron slope of -2.2 MPa/K is reasonably consistent with those determined by thermodynamic calculation (Akaogi et al., 2007) and first principles investigation (Yu et al., 2007), whereas it is inconsistent with recent experimental works which reported that the transition pressures are insensitive to temperature (Katsura et al., 2003; Fei et al., 2004). The postspinel transition pressure at 1873 K is calculated to be 22.4 GPa, which is about 1 GPa lower than that at 660 km depth, indicating effect of aluminum in pyrolitic composition to the transition pressure or uncertainty of MgO pressure scale. We can interpret topography of 660 km seismic discontinuity (plus-minus 20 km from the average) as temperature anomaly of plus-minus 370 K using the postspinel Clapeyron slope determined in the present study. The postspinel Clapeyron slope of -2.2 MPa/K can produce buoyancy for subducting slabs and the buoyancy is one of the main factors to let them stagnant on the 660-km discontinuity.

Keywords: postspinel, phase boundary, Clapeyron slope, 660 km seismic discontinuity

SIT004-09

会場:105

時間:5月25日 14:45-15:00

環太平洋深さ 400-1000 km におけるスラブ沈み込み過程 Slab subduction processes in a depth range 400-1000 km around the Circum Pacific

深尾 良夫^{1*}, 大林 政行¹

Yoshio Fukao^{1*}, Obayashi Masayuki¹

¹ 海洋研究開発機構

¹IFREE/JAMSTEC

There have been many tomographic studies to sharpen the images of deeply subducted slabs but, to our knowledge, none of them addressed the possible unique role of the uppermost lower mantle in the processes of slab subduction. We made a systematic survey of the slab images around the Circum Pacific in our P-wave tomographic model to show that a subducting slab is now in one of the following four stages:

- A. Slab is stagnant above the 660.
- B. Stagnant slab begins to penetrate the 660.
- C. Penetrated slab is trapped in the uppermost lower mantle.
- D. Trapped slab begins to penetrate well into the deep lower mantle.

We interpret A to D as the successive stages of slab subduction through the mantle transition region from 400 to 1000 km depths. In particular, we emphasize C as a distinct stage of slab subduction. Although the 660 is often interpreted as not only the boundary of phase transition but also the boundary of viscosity contrast, the distinct stage C implies that viscosity increase does not occur sharply across the 660 but gradually through the uppermost part of the lower mantle.

キーワード: マントルダイナミクス, マントル粘性

Keywords: mantle dynamics, mantle viscosity

SIT004-10

会場:105

時間:5月25日 15:00-15:30

スタグナントスラブのゆくえ：パイロライト及びスラブ物質の密度と弾性波速度からの制約

Fate of stagnant slabs: Constraints from density and sound velocities of pyrolite and subducted slab materials

入船 徹男^{1*}, 河野義生¹, 肥後祐司², 西山宣正¹

Tetsuo Irifune^{1*}, Kono Yoshio¹, Yuji Higo², Nishiyama Norimasa¹

¹ 愛媛大学地球深部研, ² 高輝度光科学研究

¹GRC, Ehime Univ., ²JASRI, SPring-8

Seismological tomography images suggest that some slabs penetrate into the deep lower mantle, while others are trapped around the 660km seismic discontinuity, forming structures referred to as "megoliths" or "stagnant slabs". The latter class of slabs is believed to eventually fall into the lower mantle, because of the instability (flushing or avalanche) caused primarily by the density contrast between the slab and the surrounding mantle. This suggests that all slab material ultimately sinks deep into the lower mantle. Nevertheless, there are some locations where the stagnant slabs seem to spread over a certain distance along the 660km boundary, whose fate is not really understood. Our recent studies on the sound velocity changes in typical subducted slab and mantle lithologies demonstrated that the sound velocities of either pyrolite or piclogite (or eclogite) do not fit seismological models for the bottom part of the mantle transition region (MTR), suggesting that this part of the MTR is made of a layer of harzburgite, which is the major constituent of subducting slabs. Subducted harzburgite is intrinsically less dense than the surrounding pyrolite in the lower mantle, and can be buoyantly trapped at the bottom of MTR when thermally equilibrated with the mantle after stagnation. This would allow such stagnant slabs to stay in this region without flushing into the deeper mantle. Thus, the authors propose that the slabs subducted in the MTR may be classified into three types; 1) directly penetrating deeper into the lower mantle, 2) forming a "megolith" structure with subsequent flushing into the lower mantle, and 3) spreading horizontally over a certain distance until some thermal turbulences (either upward or downward convective motions) destroy the layered structure. The third class of the subducted slabs, mainly composed of harzburgite, may contribute to the relatively high sound velocities observed in the bottom region of the MTR.

キーワード: スタグナントスラブ, 崩落, ハルツバージャイト, パイロライト, メガリス, マントル遷移層

Keywords: stagnant slab, flushing, harzburgite, pyrolite, megalith, mantle transition region

SIT004-11

会場:105

時間:5月25日 15:30-15:45

下部マントル最上部へ沈み込んだスラブ中で連結したフェロペリクレース Interconnected ferro-periclase in the subducting slab at the top of lower mantle

山崎 大輔^{1*}

Daisuke Yamazaki^{1*}

¹ 岡山大学

¹ Okayama University

Major phase transformation occurs from ringwoodite to (Mg,Fe)SiO₃ perovskite plus ferro-periclase when oceanic lithosphere sink into deep mantle across the 660 km discontinuity. After the transformation, material (rock) properties strongly depend on their two phase geometry, for example, grain-size, phase distribution, grain shape, lattice preferred orientation, and so on. The interconnection of ferro-periclase is a key factor on rheology and chemical heterogeneity because ferro-periclase is much weaker than (Mg,Fe)SiO₃ perovskite and chemical diffusivity of ferro-periclase is higher than that of (Mg,Fe)SiO₃ perovskite.

To investigate the interconnectivity of ferro-periclase after transformation from ringwoodite in the conditions of subducting slab, we carried out in-situ electrical conductivity measurement by means of high pressure experiment using a Kawai-type multi-anvil apparatus and 3D-textural observation on the recovered sample using FIB-SEM technique. The electrical conductivity of ferro-periclase is much higher than that of perovskite, suggesting that the conductivity of their aggregate is good indicator to estimate interconnectivity of ferro-periclase.

Our result suggested that the interconnected network of ferro-periclase was formed after phase transition from ringwoodite and remained for a while in the condition of cold subducting slab, leading that interconnected ferro-periclase plays important role on physicochemical properties of bulk rock. On the other hand, in the warm slab or regular mantle, ferro-periclase may be isolated in the aggregate. In this case, (Mg,Fe)SiO₃ perovskite mainly controls the bulk properties.

キーワード: 下部マントル, フェロペリクレース, 連結

SIT004-12

会場:105

時間:5月25日 15:45-16:15

Channel Flow in transition zone and bounds on lower-mantle lateral viscosity contrast Channel Flow in transition zone and bounds on lower-mantle lateral viscosity contrast

Yuen David^{1*}, Nicola Tosi², Z. Q. Wu³, Renata M. Wentzcovitch⁴
David Yuen^{1*}, Nicola Tosi², Z. Q. Wu³, Renata M. Wentzcovitch⁴

¹Dept. Geol. Geophys., Univ. Minnesota, ²German Aerospace Center, ³Dept. Earth and Planetary Sciences, USTC, ⁴Dept. Chem. Eng. Mater. Sci. U.Minnesota

¹Dept. Geol. Geophys., Univ. Minnesota, ²German Aerospace Center, ³Dept. Earth and Planetary Sciences, USTC, ⁴Dept. Chem. Eng. Mater. Sci. U.Minnesota

Recent high-resolution seismic imaging of the transition-zone thickness beneath the Hawaiian hotspot by the M.I.T.-Purdue group (Cao et al., 2010), using curvelet transform of multiple scattered S waves, has shown convincingly a considerable uplift of the 660 km discontinuity west of Hawaii without a correspondent depression of the 410 km discontinuity. Such a structure is consistent with the geodynamical scenario of a deep-mantle plume first deflected horizontally as a channel flow at 660 km depth and the reentrance into the upper mantle away from its lower mantle source, as a secondary plume aligned with the present-day location of the hot-spot. Using a cylindrical model of mantle convection featuring multiple phase transitions and pressure-dependent thermodynamic properties according to recent mineral physics evidence both taken experimentally and computationally, we investigate the conditions under which such a peculiar plume morphology can be realized. We have employed a temperature- and pressure-dependent thermal expansivity based on tabulated results from first-principles calculations. We focus on the magnitude $\Delta\eta_T$ of the lateral viscosity contrast due to temperature variations and show that this factor plays a first-order role on the dynamics of plumes if pressure-dependent thermal expansivity and conductivity are taken into account. For small values ($\Delta\eta_T \sim 10$), large-scale upwellings are generated at the bottom thermal boundary layer that have enough buoyancy to pass undisturbed the endothermic transition at 660 km depth in an essentially vertical fashion. For higher values ($\Delta\eta_T \sim 10^2 - 10^3$) mantle layering becomes more pronounced, plumes are thinner and weaker, still with enough buoyancy to reach the 660 km discontinuity but not to penetrate it. Instead, they travel horizontally along the 660 km boundary following the top part of lower mantle convection cells and rise again through the upper mantle at a distance from their parent plume also controlled by $\Delta\eta_T$. Our findings argue for the importance of using a temperature-dependent viscosity in numerical models that feature also pressure- and temperature-dependent thermodynamic properties and on the possibility of using plume dynamics as imaged from seismic waves to bound the temperature viscosity contrast in the lower mantle to be between one hundred and a few hundred.

Cao Q., R.D. van der Hilst, M.V. de Hoop, S. Shim. Complex plume dynamics in the transition zone underneath the Hawaii hotspot: seismic imaging results. DI23C-02, AGU Fall Meeting 2010, San Francisco.

SIT004-13

会場:105

時間:5月25日 16:30-16:45

化学的不均質と大陸移動の影響を考慮した2次元マントル対流シミュレーション Two-Dimensional numerical simulations of mantle convection with chemical heterogeneity and continental drift

亀山 真典^{1*}, 福田 将志¹

Masanori Kameyama^{1*}, Masashi Fukuda¹

¹ 愛媛大学地球深部ダイナミクス研究センター

¹ Geodynamics Research Center, Ehime Univ.

We conducted numerical experiments of mantle convection in order to study the generation of ascending plumes in the presence of chemical heterogeneity and continental drift. In this study, we consider a convection of fluid with variable physical properties such as viscosity, thermal expansivity and conductivity, under the extended Boussinesq approximation, in a model of a two-dimensional rectangular box of 2900km height and the aspect ratio (width/height) of 12. The mantle materials are modeled by a mixture of two component fluids with different density. The convecting motion of fluid is driven by not only a thermal but also a chemical buoyancy coming from the variation in the content of denser component fluid. In addition, we impose a block of highly viscous fluid of 11600km width along the top surface, as a model of a supercontinent. We also take into account the effects of a drifting motion of supercontinent, by allowing a coherent (rigid) motion of continental block in the horizontal direction driven by the overall convection in the mantle. Our preliminary calculations showed that, when the effect of negative chemical buoyancy is sufficiently large, several dome-like structures of dense materials occur at the base of the mantle. The dome-like structures form broad regions of high temperature, which are quite similar to the large low shear-velocity provinces (LLSVPs) in the lowermost mantle of the Earth.

Our calculations demonstrated that the thermal and chemical state in the deep mantle described above is significantly affected by the presence of the continental block at the top surface. In particular, owing to a strong “blanketing effect”, both thermally and chemically, caused by the continental block, a pile of dense and hot materials firmly develops beneath the initial position of the continent. The thermochemical pile, once it forms beneath the continental block, remains strong enough to dominate the overall convection in the mantle, causing intense ascending flows in its neighborhood. In addition, we found that, only when an appropriate amount of high density component (around 10% of the entire volume) is present in the mantle, convective flows can simultaneously yield the occurrence of continental drift and the long-term survival of LLSVPs.

Furthermore, from the observations of the temporal variations in convective planforms, we found that the thermochemical pile beneath the initial continental position is almost immobile for more than several gigayears: The pile of dense material remains stationary even after the continental block is swept away by the ascending flows originating from the root of the pile. This finding suggests that, considering the effect of chemical heterogeneity, the cycles of aggregation/dispersal of supercontinents are not necessarily associated with cyclic changes in convection patterns in the mantle, as opposed to the “1-2-1 model” proposed by Zhong et al. (2007).

キーワード: マントル対流, 数値シミュレーション, 化学不均質, 超大陸サイクル, LLSVP, 上昇ブルーム

Keywords: mantle convection, numerical simulation, chemical heterogeneity, supercontinent cycle, LLSVP, ascending plume

SIT004-14

会場:105

時間:5月25日 16:45-17:00

Effects of iron on the thermoelastic properties of MgSiO_3 perovskite Effects of iron on the thermoelastic properties of MgSiO_3 perovskite

Arnaud Metsue^{1*}, Taku Tsuchiya¹

Arnaud Metsue^{1*}, Taku Tsuchiya¹

¹Geodynamic Research Center, Ehime

¹Geodynamic Research Center, Ehime

$(\text{Mg,Fe})\text{SiO}_3$ perovskite is thought to be the most abundant phases in the Earth lower mantle. Mineral physical studies on this phase is therefore of significant importance in investigating structure and dynamics of the Earth deep mantle. However, due to some technical difficulties for the iron-bearing phases, its high-P,T thermodynamics are yet to be well understood both experimentally and theoretically. In particular, all the ab initio studies on $(\text{Mg,Fe})\text{SiO}_3$ perovskite conducted so far are limited at the static condition in contrast to pure MgSiO_3 .

Here, we present the results of a computational study on the thermodynamic properties of Fe-bearing MgSiO_3 perovskite up to 150GPa. We perform density functional calculations beyond conventional methods based on the internally consistent LDA+U technique (Tsuchiya et al., 2006, Phys. Rev. Lett.) to describe local interactions between the d-states in Fe in more appropriately, that give rise to Hubbard splitting. In this study, Fe is incorporated as substitutional single-point defects, which can be present in the different oxidation states (+2 or +3) and different spin states (low or high). We calculate the phonon dispersion relations of the iron-bearing phases based on the direct method, where the force constant matrices are determined by directly applying small but finite atomic displacements, similarly to our previous study in Fe-bearing MgSiO_3 post-perovskite (Metsue and Tsuchiya, 2011, under review). Then, we determine several important thermodynamic quantities such as the vibrational entropy, free energy, heat capacities, bulk moduli and thermal expansion coefficient within the quasiharmonic approximation. These results are compared to those reported by Tsuchiya et al. (2005, J. Geo. Res.) for pure MgSiO_3 perovskite. In addition, we show that our results are in good agreement with previous experimental studies on Fe-bearing perovskite (Andrault et al., 2001, EPSL; Lundin et al., 2008, PEPI; Catalli et al., 2010, EPSL). This study points the fact that a low concentration of iron, irrespective of the spin state, affects mainly the low phonon frequency ranges of the perovskite and thus has limited effects on its thermodynamic properties.

Research supported by the Ehime Univ. G-COE program Deep Earth Mineralogy and JSPS Research Grants Nos. 20001005 and 21740379.

キーワード: perovskite, equation of states, thermodynamic properties, phonon spectra, first-principle calculations

Keywords: perovskite, equation of states, thermodynamic properties, phonon spectra, first-principle calculations

SIT004-15

会場:105

時間:5月25日 17:00-17:30

The Importance of Mineral Physics for Understanding Mantle Dynamics and Seismic Structure

The Importance of Mineral Physics for Understanding Mantle Dynamics and Seismic Structure

Paul Tackley^{1*}, Takashi Nakagawa¹, Frederic Deschamps¹, James Connolly¹
Paul Tackley^{1*}, Takashi Nakagawa¹, Frederic Deschamps¹, James Connolly¹

¹Dept. Earth Sciences, ETH Zurich, ².

¹Dept. Earth Sciences, ETH Zurich, ².

Phase transitions have a first-order influence on the mantle, yet mantle dynamics calculations typically only include one or two major transitions despite the complexity of phase diagrams for mantle mineralogy. In our recent work, phase assemblages of mantle rocks calculated from the ratios of six oxides (CaO-FeO-MgO-Al₂O₃-SiO₂-Na₂O) by free energy minimization are used to calculate the material properties density, thermal expansivity, specific heat capacity, and seismic velocity as a function of temperature, pressure, and composition, which are incorporated into a numerical thermochemical mantle convection model in a 3-D spherical shell. The advantage of using such an approach is that thermodynamic parameters affecting dynamics and seismic velocities are included implicitly and self-consistently, obviating the need for ad hoc parameterizations. We test the sensitivity of convective behaviour and resulting mantle structure to the compositions of mid ocean ridge basalt (MORB) and harzburgite. Results indicate that thermo-chemical structures are quite sensitive to variations in MORB composition of the order 1-2% oxide fraction, particularly FeO and Al₂O₃. Differences occur in (i) the amount of compositional stratification around 660 km depth caused by the inversion of the MORB-harzburgite density difference between about 660 - 740 km depth, which is different in magnitude and depth extent between the different tested compositions, and (ii) in the degree of MORB segregation above the CMB, which is related to differences in the MORB-harzburgite density difference in the deep mantle. Comparing model spectra to those of seismic tomography, in all cases there is too much heterogeneity at mid lower mantle depths compared to typical seismic tomographic models, which implies that less CMB basalt segregation occurs in Earth than in the models. This probably indicates the need for better thermodynamic data for minerals at deep mantle pressures and temperatures.

キーワード: mantle convection, plate tectonics, mineral physics, numerical simulation

Keywords: mantle convection, plate tectonics, mineral physics, numerical simulation

SIT004-16

会場:105

時間:5月25日 17:30-18:00

パイロライト的な下部マントルの密度プロファイル Density profile of pyrolitic lower mantle

新名 良介^{2*}, 廣瀬 敬¹, 大石 泰生³

Ryosuke Sinmyo^{2*}, Kei Hirose¹, Yasuo Ohishi³

¹ 東京工業大学, ² パイロイト大学, ³ 財団法人高輝度光科学研究センター

¹Tokyo Institute of Technology, ²Universitaet Bayreuth, ³JASRI

Density profile of pyrolite at lower mantle high-pressure (P) and -temperature (T) conditions was investigated by using laser-heated diamond-anvil cell up to 117 GPa and 2800 K. The density was determined from chemical composition and unit-cell volume of each constituent mineral (MgSiO₃-rich perovskite, ferropericlaase and CaSiO₃-rich perovskite). The chemical compositions of coexisting phases were analyzed by transmission electron microscope, and their volumes were obtained by in-situ X-ray diffraction measurements. To avoid extensive chemical segregation during laser-heating, sample was coated by gold that worked as a laser absorber (Sinmyo and Hirose 2010 PEPI). Results of chemical analyses show that Mg-Fe (total Fe) partitioning coefficient between MgSiO₃-rich perovskite and ferropericlaase [$K^* = (Fe^*/Mg)_{Pv}/(Fe^*/Mg)_{Fp}$] is about 0.6, slightly higher than the value previously reported in the pyrolitic bulk composition (Murakami et al. 2005). The lower K^* value in the previous study may be attributed to the chemical heterogeneity in the sample induced by strong temperature gradient during laser heating. The calculated density profile of pyrolite is indeed in good agreement with the PREM model within experimental errors, in contrast with the mismatch reported by the previous study (Ricolleau et al. 2009). Our results support the lower mantle has pyrolitic bulk composition, and thus it is not necessary to suppose the chemically stratification in the lower mantle.

SIT004-17

会場:105

時間:5月25日 18:00-18:15

低粘性ポストペロブスカイトを考慮した3次元球殻熱化学マントル対流モデルによるマントル深部への力学的な影響

Dynamical response of the low viscosity post-perovskite in thermo-chemical mantle convection in a 3-D spherical shell

中川 貴司^{1*}, Tackley Paul¹

Takashi Nakagawa^{1*}, Paul Tackley¹

¹ スイス連邦工科大学チューリッヒ校

¹Institute of Geophysics, ETH Zurich

Both high pressure experiment and theory suggested that the rheological property of post-perovskite phase could be much weaker than of perovskite, which could have $O(10^{-3})$ to $O(10^{-4})$ [Hunt et al., 2009; Ammann et al., 2010]. Recent our study indicated that the scale of heat flux across the core-mantle boundary and thermo-chemical anomalies were the larger-scale when the post-perovskite is weaker than the perovskite [Nakagawa and Tackley, 2011]. Other important physical response caused by the low viscosity post-perovskite is to check the geoid anomalies and anisotropic features induced by flow in the post-perovskite phase. Several previous studies indicated that the viscosity reduction due to the post-perovskite phase transition could affect the large-scale geoid anomalies [Tosi et al., 2009; Gosh et al., 2010]. In addition, high pressure mineral physics also implied that the weak post-perovskite could induce the anisotropic feature in the deep mantle [Yamazaki et al., 2006; Shim, 2008]. Here we test two important physical response caused by the low viscosity post-perovskite in thermo-chemical mantle convection simulations in a 3-D spherical shell varying the density difference at the core-mantle boundary that would affect thermo-chemical structures in the deep mantle. Comparing between the weaker post-perovskite and regular post-perovskite, the amplitude of geoid anomalies is not very different but the scale of geoid would be somewhat organized to be the larger-scale when the viscosity of post-perovskite is weaker than of perovskite. The anisotropic structure would also affect to enhance the horizontal flow structure then making an alignment to the horizontal direction when the low viscosity post-perovskite is assumed, which could be related to the anisotropic structure in the deep mantle.

Keywords: Postperovskite, thermochemical mantle convection, geoid, anisotropy

SIT004-18

会場:105

時間:5月25日 18:15-18:30

ソサエティーホットスポット（仏領ポリネシア）付近での海底地球物理観測 Ocean bottom geophysical observation on the seafloor near the Society hot spot, French Polynesia

末次 大輔^{1*}, 塩原 肇², 杉岡 裕子¹, 伊藤 亜妃¹, 一瀬 建日², 馬場 聖至², 笠谷 貴史¹, 多田 訓子¹

Daisuke Suetsugu^{1*}, Hajime Shiobara², Hiroko Sugioka¹, Aki Ito¹, Takehi Isse², Kiyoshi Baba², Takafumi Kasaya¹, Noriko Tada¹

¹ 海洋研究開発機構, ² 東京大学地震研究所

¹IFREE/JAMSTEC, ²ERI/Univ. Tokyo

The South Pacific region is characterized by a broadly elevated seafloor known as the South Pacific superswell, which suggests the presence of a large-scale mantle plume beneath the South Pacific, called the South Pacific superplume. The geometry, origin depth, temperature, and composition of the superplume remain controversial, however, mainly due to the lack of seismological data that documents the mantle structure beneath the South Pacific. To obtain a better seismic image of the superplume, we deployed temporary broadband seismographs on oceanic islands and the seafloor in the South Pacific since 2002. In the first experiment from 2002-2005, we deployed 10 broadband ocean-bottom seismographs (BBOBS) over the French Polynesian region. The seismic image obtained from the data indicates that large-scale low-velocity anomalies (on the order of 1000 km in diameter), indicative of the superplume, are located from the bottom of the mantle to a depth of 1000 km, and small-scale low-velocity anomalies (on the order of 100 km in diameter) are present above it. The small-scale anomalies may be narrow plumes generated from the top of the dome. Narrow plumes beneath the Society hot spot are best resolved by the data, although the spatial resolution is still not sufficient to understand how the narrow plumes reach from the top of the superplume to the hot spot. In the second experiment from Feb. 2009 to Dec. 2010, we deployed 9 BBOBS and 9 ocean-bottom electro-magnetometers (OBEM) near the Society hot spot to obtain a clear image of the ascending narrow plumes beneath the hot spot. Simultaneous observation with seismic and electro-magnetic sensors should enable not only to determine geometry of the plumes, but also to investigate thermal and compositional heterogeneities associated with the plumes. The observation was planned and conducted by a Japan-France research collaboration. The installation and recovery of the BBOBS and OBEM were carried out with the JAMSTEC research vessel MIRAI and the Tahitian tuna-fishing boat FETU MANA, respectively. The observation was successfully completed and the 1.5 year-long data were recovered. In the session, we will present an overview of the observation and data and very initial results of the 2009-2010 data.

キーワード: 海底観測, ホットスポット

Keywords: Ocean bottom observation, hot spot